Journal of Instrumentation

PAPER • OPEN ACCESS

Development of dual X-mode Doppler reflectometry system in Heliotron J

To cite this article: Y. Kondo *et al* 2022 *JINST* **17** C05023

Published by IOP Publishing for Sissa Medialab

Received: *September 14, 2021*
Revised: *November 28, 2021*
Accepted: *February 1, 2022*
Published: *May 25, 2022*

4th European Conference on Plasma Diagnostics (ECPD2021)
7–11 June, 2021
Online

Development of dual X-mode Doppler reflectometry system in Heliotron J

Y. Kondo,[a,*] S. Ohshima,[b] D. Kuwahara,[c] K. Inoshita,[a] T. Fukuda,[d,†] T. Minami,[b] S. Kado,[b] S. Kobayashi,[b] S. Konoshima,[b] T. Mizuchi,[b] H. Okada,[b] T. Tomita[a] and K. Nagasaki[b]

[a] *Graduate School of Energy Science, Kyoto University, Uji 611-0011, Japan*
[b] *Institute of Advanced Energy, Kyoto University, Uji 611-0011, Japan*
[c] *College of Engineering, Chubu University, Kasugai 487-8501, Japan*
[d] *Graduate School of Engineering, Osaka University, Suita 565-0871, Japan*

E-mail: kondou.yasuto.72d@st.kyoto-u.ac.jp

Abstract: A dual X-mode Doppler reflectometry system is developed to measure the radial electric field in a stellarator/heliotron device, Heliotron J. The system is designed to have dual channels where the observation points are placed symmetrically to the equatorial plane, enabling the poloidal flow velocity measurement at two different positions in the same toroidal section, which is useful for the search for a zonal flow. In the system, an RF source generates the microwave frequency of 8.25–12.5 GHz, upconverted by an intermediate frequency of 27.5 MHz and transmitted with a coaxial cable to a transmitter located near the Heliotoron J vacuum vessel. After quadrupling the RF waves at the transmitter, the microwaves of 33–50 GHz are injected in X-mode into a plasma using a spherical focusing mirror installed inside the vacuum vessel. The local wavenumber of the probing microwaves, $k_\perp$, is 1.56–1.66 cm^{-1}. The Doppler-shifted reflected wave is downconverted to a 110 MHz signal by mixing with the LO at the receiver, amplified, and then detected by an I/Q detector. In a tabletop test, we have confirmed that the phase estimated by the I/Q detector is proportionally changed as a function of the horn antenna distance. We have successfully measured the Doppler-shifted spectra of the I/Q signals and estimated the radial electric field in an electron cyclotron heated (ECH) plasma.

*Corresponding author.
†Deceased.

https://doi.org/10.1088/1748-0221/17/05/C05023

2022 JINST 17 C05023

Keywords: Plasma diagnostics — interferometry, spectroscopy and imaging; Nuclear instruments and methods for hot plasma diagnostics

Contents

1 Introduction

In magnetically confined fusion plasmas, turbulent transport dominates the confinement, and the radial electric field, E_r, and zonal flows (ZF) play a critical role in turbulent transport and confinement properties. It is therefore recognized that the measurement of E_r and ZF contributes to understanding the physics of plasma confinement. Doppler reflectometry is a powerful diagnostic to measure density fluctuation and poloidal flow velocity, $v_\perp$, (or E_r) simultaneously, with high temporal and spatial resolution in high-temperature plasmas. It is used in worldwide fusion devices such as tokamaks (ASDEX Upgrade [1, 2], DIII-D [3], JT-60U [4]) and stellarator/heliotron (Wendelstein 7-AS [5], Wendelstein 7-X [6], TJ-II [7], LHD [8], Heliotron J [9, 10]) and has great contributions to the measurement of turbulence and E_r on plasma dynamics such as L-H transition. In Heliotron J, Langmuir probes have been used to search for ZF [11], and in this study, a dual Doppler reflectometry system is newly introduced to extend the parameter and operation space for turbulence and ZF studies. An O-mode Doppler reflectometry system has been operated for poloidal flow and radial electric field measurements since 2019 [9]. Although we estimated the radial electric field with this system, we had the following problems: it was not suitable for local radial electric field measurements because the incident microwaves were not focused using mirrors, and the cut-off density was $0.84\text{–}1.98 \times 10^{19}\ \mathrm{m}^{-3}$, which is challenging to apply to ECH plasmas with hollow density profiles of Heliotron J, and the measurement at two different poloidal angles is not possible. In this paper, we report the development of the dual Doppler reflectometry system for local measurement using a focusing mirror and X-mode incidence, which can be applied to typically ECH plasmas with hollow or flat density profiles in the Heliotron J device.

2022 JINST 17 C05023

2 Experimental setup

2.1 Measurement principle of Doppler reflectometry

In Doppler reflectometry, the probing microwave is obliquely injected to the cut-off layer at an angle θ_D, and the scattered microwave is Doppler shifted. The shifted frequency can be expressed as $f_D = v_\perp k_\perp / 2\pi = 2 v_\perp k_0 \sin\theta_D / \pi$, where $v_\perp$, $k_\perp$, and k_0 are the poloidal fluctuation propagation velocity, the fluctuation wavenumber, and the probing microwave wavenumber in a vacuum, respectively [5]. The shifted frequency corresponds to the poloidal flow velocity of fluctuation. Since $v_\perp = v_{E\times B} + v_{ph}$, where $v_{E\times B}$ is the $E \times B$ drift velocity and v_{ph} is the phase velocity of the fluctuation, E_r can be evaluated if $v_{E\times B} \gg v_{ph}$ can be assumed.

2.2 Dual Doppler reflectometry system in Heliotron J

The Doppler reflectometry system has been installed in a medium-sized stellarator/heliotron device, Heliotron J, with major/minor radii, R/a = 1.2 m/0.1–0.2 m and the magnetic field strength B = 1.5 T on magnetic axis [12, 13]. Figure 1 shows the schematic of the Q-band (33–50 GHz) dual Doppler reflectometry system. The system can measure $v_\perp$ at two symmetrical positions to the equatorial plane simultaneously in the same toroidal section by using the upper and the lower antenna systems installed inside the vacuum vessel. This article refers to the upper and lower antenna as "upper channel" and "lower channel." The arrangement of the dual-channel is aimed at searching for ZF based on correlation analysis. The microwaves launched from antennas are focused by spherical mirrors with a curvature radius, R = 120 mm, and injected in X-mode into the plasmas. The injection angle is fixed at about 10 degrees with respect to the LCFS. For a typical ECH plasma of Heliotron J, the wavenumbers of the probing microwaves are calculated by the ray-tracing code TRAVIS [14]. Figure 2 shows the density profile used for the ray-tracing calculations and the wavenumber for microwave frequencies ranging from 33 to 39 GHz at upper channel. The cut-off region is r/a = 0.907 to 0.966, and the wavenumber range is $k_\perp$ = 1.56 to 1.66 cm^{-1}. $\Delta k_\perp$ evaluated by ray-tracing calculation considering $1/e$ finite beamwidth of microwaves [7, 15] is 0.776 to 4.38 cm^{-1}, and the relative error is 0.488 to 0.726. The measurement position was located at a place where the magnetic surface curvature is large, therefore, the difference in the microwave injection angle θ_D at the center and both edges of the incident beam was large. In the future, we will improve the position and the tilt angle of the focusing mirror to optimized one so that the microwaves will be incident on a position with low magnetic surface curvature.

2.3 Microwave circuits

As shown in figure 1, a voltage-controlled oscillator (VCO) is used for the frequency source of the Doppler reflectometry system, which generates microwaves of 8.25–12.5 GHz (PreRF). VCO output has no filtering devices from the following reasons: Since the frequency of X-band VCO output is variable from 8.25 to 12.5 GHz, BPF with a fixed bandwidth cannot be used. The microwaves are upconverted by an IQ mixer with an intermediate frequency of 27.5 MHz generated by XO, so there is at least 16 dB difference between the 8 to 12.5 GHz + 27.5 MHz and the unwanted

2022 JINST 17 C05023

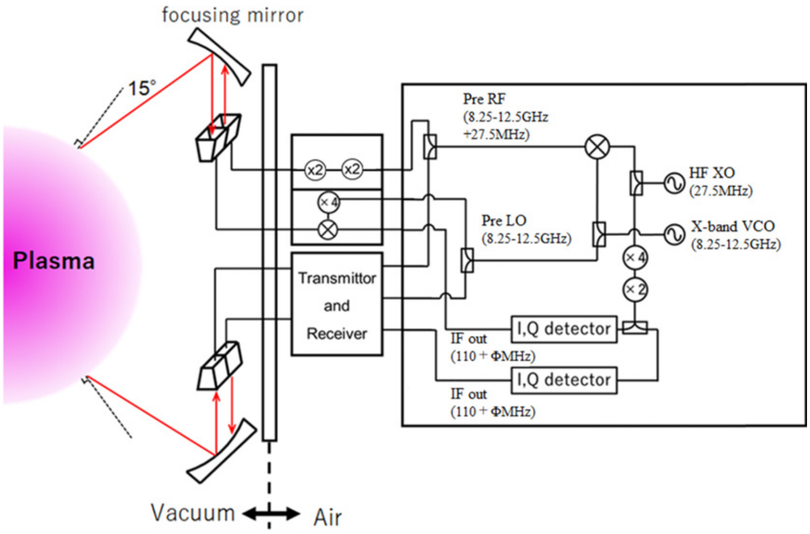

Figure 1. Schematic of the dual Doppler reflectometer system in the Heliotron J.

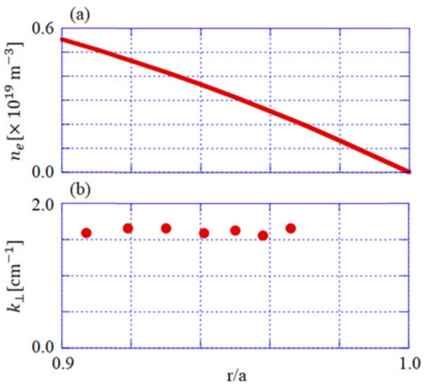

Figure 2. (a) Assumed electron density profile and (b) $k_\perp$ as a function of r/a calculated by ray-tracing code.

hramonic components. Although unwanted harmonic components are generated at intervals of 27.5 MHz, the I/Q detector (“LT5502” from analog devices) which has an IF bandwidth with 7.7 MHz is not sensitive to them. The upconverted microwaves are transmitted by a coaxial cable to a transmitter located near the Heliotron J vacuum vessel. After the transmitter quadruples the microwaves, the microwaves of 33–50 GHz contain sideband frequencies. However, their effect on the measurement is small since they are about 20–30 dBm lower in power than the main frequency. The microwaves of 33–50 GHz are focused by a spherical focusing mirror through a coaxial-to-waveguide converter, waveguide E-bends, waveguide twists and horn antenna installed in the vacuum vessel and injected in X-mode into the plasma. These components installed in the vacuum vessel are more than 15 cm away from the plasma. The possibility of damage due to X-rays or heat load is low because the Heliotron J produces few neutrons, and the discharge time is short, less than 200 ms. The Doppler-shifted scattered wave is downconverted to a 110 MHz signal by mixing with the LO at the receiver, amplified, and then detected by an I/Q detector. The I/Q detector operating at 220 MHz LO is used to avoid the interference with 110 MHz IF.

The transmission system features are a multiplier inside the transmitter and receiver for high frequency up/down conversion, and V-connector vacuum feedthrough (shown in figure 3) to enable the use of coaxial cables. The V-connector is a commercial coaxial connector standard that can be used in the frequency range from DC to 65 GHz, and the in-house made feedthrough has a 1 dB loss in the 30–50 GHz. The transmitter and receiver are located near the vacuum vessel, and the transmission line up to the transmitter and receiver is about 11 meters long. It consists of coaxial cables, which transmit low-frequency band waves, resulting in low loss and easy handling [16, 17]. On the other hand, the transmitter and receiver near the vacuum vessel are prone to failure due to the high voltage and noise of the Heliotron J vacuum vessel. This problem is addressed by insulating them from the vacuum vessel. The transmitter and receiver have been newly developed by Microwave Monolithic Integrated Circuit (MMIC). The transmitter consists of two multipliers HMC814 and HMC579, with different bandwidths, and the receiver consists of an MMIC with an integrated quadrupler and mixer, HMC1093.

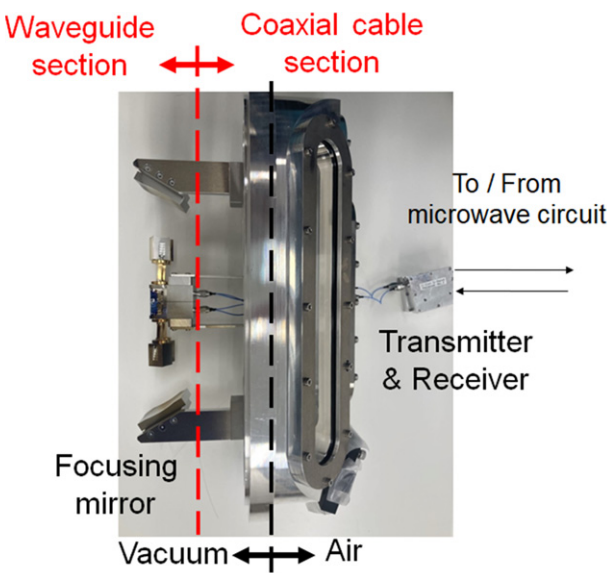

Figure 3. Photo of antenna and vacuum feedthrough for the dual Doppler reflectometer system. The photo shows only one set of transmitter/receiver for upper channel, but in reality, the other set is installed on the lower channel.

3 Experimental results

3.1 Tabletop test of new reflectometry system

Before installing the new reflectometry system to the Heliotron J, the system has been tested in a tabletop experiment. The transmitter and the receiver with horn antennas are placed in a straight line, and the phase change evaluated from the I/Q detected signal ($\varphi = \tan^{-1}(Q/I)$) is measured by varying the distance between them. The spatial resolution of the measurement is 0.2 mm.

2022 JINST 17 C05023

Although the microwave phase is slightly distorted around $\pm\pi/2$, the evaluated wavelength is 6.667 mm at 44.80 GHz, which is 0.42% error from the ideal value of 6.695 mm. Similar results are obtained at other frequencies such as 33.50 GHz and 39.70 GHz, demonstrating that the system is working properly.

3.2 E_r profile measurement in Heliotron J

An initial measurement has been tried using the new Doppler reflectometry system in Heliotron J. Figure 4(a) shows the typical plasma parameters in the ECH plasma. The E_r is measured at 230 ms (broken line in figures 4(a) and (b)). The complex Fourier spectrogram obtained from the Doppler reflectometry I/Q signals is shown in figure 4(b) (as a representative from a series of fixed shots, #78903), which shows asymmetry in the spectrum around 230 ms due to Doppler shift.

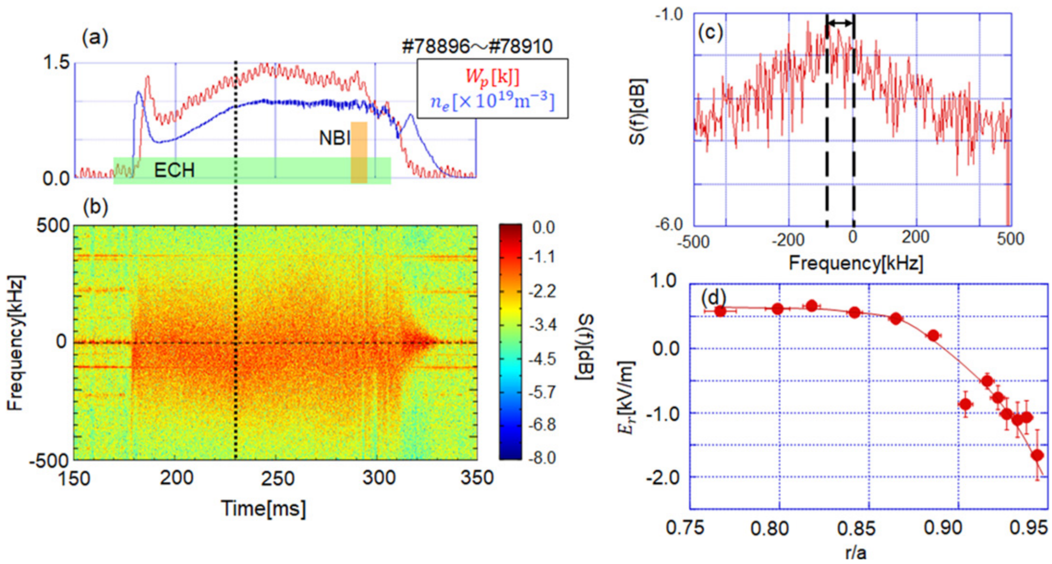

Figure 4. (a) Typical ECH plasma discharge (#78903), (b) reflectometer spectrogram (#78903), (c) complex Fourier spectrum at 230 ms (#78903), and (d) estimated E_r profile at 230 ms (#78896 ~ #78910).

An asymmetric peak due to Doppler shift can be seen around −100 kHz clearly, as shown in the complex Fourier spectrum of figure 4(c) at 230 ms. Here, Doppler-shifted frequency is evaluated with the Center-of-Gravity method (CoG) defined as $f_D = \sum(f \cdot S(f)) / \sum S(f)$, where f is the frequency in complex Fourier spectrum and $S(f)$ is the intensity at f. The evaluated f_D is -71.33 ± 5.73 kHz. The cut-off position, r/a, and B_t at the cut-off obtained by the ray-tracing code, TRAVIS, are 0.94 and 0.96 T, respectively. Therefore, from the equations $f_D = 2v_\theta k_0 \sin\theta_D/\pi$ and $E_r = v_\theta B_t$, v_θ and E_r are 1.42 km/s and 1.36 kV/m, respectively.

Figure 4(d) shows the E_r profile obtained with the Doppler reflectometry by changing the carrier microwave frequency shot by shot in fixed plasma conditions. The carrier microwave frequencies are 36.89–45.74 GHz, which correspond to cut-off positions of r/a = 0.82–0.94. A positive E_r is observed inside the plasma and a negative E_r is observed outside the plasma. E_r changes the sign at $r/a \sim 0.9$.

3.3 Dual measurement

The simultaneous measurement of E_r with the dual channels has been successfully conducted, as shown in figure 5. The time trace of ECH plasma discharge (#78752) is shown in figure 5(a). Figures 5(b) and (c) show the time evolutions of f_D measured with the upper and lower channels, respectively. The temporal behavior of E_r are similar, but not identical since the observation points for upper and lower channels are different. This may be due to misalignment of the dual channels from the ideal position, caused by the three-dimensionality of the Heliotron J configuration. We will improve the measurement accuracy by considering the magnetic configuration.

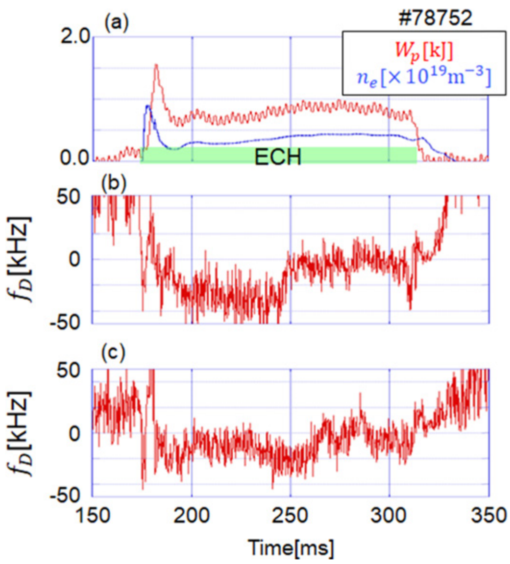

Figure 5. (a) ECH plasma discharge, and time evolution of f_D of (b) upper channel, $r/a = 0.51$ and (c) lower channel, $r/a = 0.26$.

4 Conclusion

We have introduced the newly developed dual Doppler reflectometry system in the Heliotron J device. The main feature of this system is that it can simultaneously measure two points with different poloidal angles in the same toroidal section. The tabletop test has confirmed that the phase estimated from the I/Q detector is proportionally changed as a function of the antenna distance, indicating that the system works properly. In the initial ECH plasma experiment, we have measured the Doppler-shifted spectra of the I/Q signals and estimated the E_r and dual Doppler shift measurement. The frequency scan shows that E_r is negative at the plasma edge with a negative shear structure. In the future experiment, we will identify ZF using correlation analysis and measure detailed radial E_r structure by scanning the carrier frequency.

Acknowledgments

The authors thank the Heliotron J staff for conducting the plasma experiments. This study was carried out with the support of the NIFS Collaborative Research Program (NIFS10KUHL030, NIFS18KUHL082, and NIFS18KUHL086), JSPS KAKENHI Grant Numbers JP20K03901, 18H01199, JST SPRING, Grant Number JPMJSP2110 and 'PLADyS', JSPS Core-to-Core Program, A. Advanced Research Networks.

References

[1] G.D. Conway et al., *Plasma rotation profile measurements using Doppler reflectometry*, *Plasma Phys. Controlled Fusion* **46** (2004) 951.

[2] J. Schirmer et al., *Radial correlation length measurements on ASDEX Upgrade using correlation Doppler reflectometry*, *Plasma Phys. Controlled Fusion* **49** (2007) 1019.

[3] J.C. Hillesheim et al., *A multichannel, frequency-modulated, tunable Doppler backscattering and reflectometry system*, *Rev. Sci. Instrum.* **80** (2009) 083507.

[4] N. Oyama et al., *Density fluctuation measurements using a frequency hopping reflectometer in JT-60U*, *Plasma Fusion Res.* **6** (2011) 1402014.

[5] M. Hirsch, E. Holzhauer, J. Baldzuhn, B. Kurzan and B. Scott, *Doppler reflectometry for the investigation of propagating density perturbations*, *Plasma Phys. Controlled Fusion* **43** (2001) 1641.

[6] T. Windisch et al., *W-band Doppler reflectometry at Wendelstein 7-X: diagnostic setup and initial results*, *2019 Proc. 14th Int. Reflectometry Wksh—IRW14*, 22–24 May 2019, https://www.aug.ipp.mpg.de/IRW/IRW14/papers/207-IRW14-Windisch-paper.pdf, Lausanne no. O.207.

[7] T. Happel et al., *Doppler reflectometer system in the stellarator TJ-II*, *Rev. Sci. Instrum.* **80** (2009) 073502.

[8] T. Tokuzawa et al., *Ka-band microwave frequency comb Doppler reflectometer system for the large helical device*, *Plasma Fusion Res.* **9** (2014) 1402149.

[9] Y. Kondo et al., *Measurement of radial electric field using Doppler reflectometer in high-density plasma of heliotron J*, *Plasma Fusion Res.* **15** (2020) 2402064.

[10] N. Smith et al., *Measurement of radial correlation lengths of electron density fluctuations in heliotron J using O-mode reflectometry*, *Plasma Fusion Res.* **15** (2020) 1202054.

[11] S. Ohshima et al., *Isotope effect on zonal flow and its configuration dependence in low-density electron-cyclotron-resonance heated plasmas in Heliotron J*, *Plasma Phys. Controlled Fusion* **63** (2021) 104002.

[12] M. Wakatani et al., *Study of a helical axis heliotron*, *Nucl. Fusion* **40** (2000) 569.

[13] T. Obiki et al., *First plasmas in heliotron J*, *Nucl. Fusion* **41** (2001) 833.

[14] N.B. Marushchenko, Y. Turkin and H. Maassberg, *Ray-tracing code TRAVIS for ECR heating, EC current drive and ECE diagnostic*, *Comput. Phys. Commun.* **185** (2014) 165.

[15] C. Zhou et al., *Microwave Doppler reflectometer system in the experimental advanced superconducting tokamak*, *Rev. Sci. Instrum.* **84** (2013) 103511.

[16] D. Kuwahara et al., *Development of horn antenna mixer array with internal local oscillator module for microwave imaging diagnostics*, *Rev. Sci. Instrum.* **85** (2014) 11D805.

[17] D. Kuwahara et al., *Development of local oscillator integrated antenna array for microwave imaging diagnostics*, 2015 *JINST* **10** C12031.

2022 JINST 17 C05023